

Discovery of [(2*R*,5*R*)-5-{{(5-Fluoropyridin-2-yl)oxy]methyl}-2-methylpiperidin-1-yl}[5-methyl-2-(pyrimidin-2-yl)phenyl]methanone (MK-6096): A Dual Orexin Receptor Antagonist with Potent Sleep-Promoting Properties

Paul J. Coleman,*^[a] John D. Schreier,^[a] Christopher D. Cox,^[a] Michael J. Breslin,^[a] David B. Whitman,^[a] Michael J. Bogusky,^[a] Georgia B. McGaughey,^[b] Rodney A. Bednar,^[c] Wei Lemaire,^[c] Scott M. Doran,^[d] Steven V. Fox,^[d] Susan L. Garson,^[d] Anthony L. Gotter,^[d] C. Meacham Harrell,^[d] Duane R. Reiss,^[d] Tamara D. Cabalu,^[e] Donghui Cui,^[e] Thomayant Prueksaritanont,^[e] Joanne Stevens,^[d] Pamela L. Tannenbaum,^[d] Richard G. Ball,^[f] Joyce Stellabott,^[g] Steven D. Young,^[a] George D. Hartman,^[a] Christopher J. Winrow,^[d] and John J. Renger^[d]

Insomnia is a common disorder that can be comorbid with other physical and psychological illnesses. Traditional management of insomnia relies on general central nervous system (CNS) suppression using GABA modulators. Many of these agents fail to meet patient needs with respect to sleep onset, maintenance, and next-day residual effects and have issues related to tolerance, memory disturbances, and balance. Orexin neuropeptides are central regulators of wakefulness, and orexin antagonism has been identified as a novel mechanism for treating insomnia with clinical proof of concept. Herein we describe the discovery of a series of α -methylpiperidine car-

boxamide dual orexin 1 and orexin 2 receptor ($\text{OX}_1\text{R}/\text{OX}_2\text{R}$) antagonists (DORAs). The design of these molecules was inspired by earlier work from this laboratory in understanding preferred conformational properties for potent orexin receptor binding. Minimization of 1,3-allylic strain interactions was used as a design principle to synthesize 2,5-disubstituted piperidine carboxamides with axially oriented substituents including DORA 28. DORA 28 (MK-6096) has exceptional *in vivo* activity in pre-clinical sleep models, and has advanced into phase II clinical trials for the treatment of insomnia.

Introduction

Insomnia is defined by difficulty in initiating sleep, maintaining sleep, or finding sleep to be non-restorative. It is a common disorder that affects 10–15% of the general population, with a higher incidence among the elderly.^[1] Insomnia is also associated with other diseases including depression, cardiovascular disease, and chronic pain.^[2] The total direct and indirect costs associated with insomnia are projected at greater than \$100 billion per year in the US.^[3] Current regimens for treating insomnia involve the use of central nervous system (CNS) depressants^[4] that modulate GABA receptor function and are associated with risks of dependence, next-day residual effects, amnesia, rebound insomnia, and myorelaxation.^[5] Given the limitations of current treatments, novel approaches that address both sleep onset and maintenance while providing excellent tolerability are needed.

Orexin neuropeptides were discovered in 1998 by two independent research groups and found to bind to the previously identified orphan G-protein-coupled receptors (GPCRs): orexin 1 receptor (OX_1R) and orexin 2 receptor (OX_2R).^[6] Orexin-secreting neurons are localized in the hypothalamus, and both orexins A and B are proteolytically derived from a common prepro-orexin peptide. The neuropeptide receptors have dis-

[a] Dr. P. J. Coleman, J. D. Schreier, Dr. C. D. Cox, M. J. Breslin, D. B. Whitman, Dr. M. J. Bogusky, Dr. S. D. Young, Dr. G. D. Hartman
Departments of Medicinal Chemistry, Merck Research Laboratories
P.O. Box 4, Sumneytown Pike, West Point, PA 19486 (USA)
E-mail: paul_coleman@merck.com

[b] Dr. G. B. McGaughey
Chemistry Modeling and Informatics, Merck Research Laboratories
P.O. Box 4, Sumneytown Pike, West Point, PA 19486 (USA)

[c] Dr. R. A. Bednar, W. Lemaire
In Vitro Sciences, Merck Research Laboratories
P.O. Box 4, Sumneytown Pike, West Point, PA 19486 (USA)

[d] Dr. S. M. Doran, S. V. Fox, S. L. Garson, Dr. A. L. Gotter, C. M. Harrell, D. R. Reiss, J. Stevens, Dr. P. L. Tannenbaum, Dr. C. J. Winrow, Dr. J. J. Renger
Neuroscience Research, Merck Research Laboratories
P.O. Box 4, Sumneytown Pike, West Point, PA 19486 (USA)

[e] Dr. T. D. Cabalu, Dr. D. Cui, Dr. T. Prueksaritanont
Drug Metabolism and Pharmacokinetics, Merck Research Laboratories
P.O. Box 4, Sumneytown Pike, West Point, PA 19486 (USA)

[f] Dr. R. G. Ball
Department of Pharmaceutical Research, Merck Research Laboratories
P.O. Box 2000, 126 E. Lincoln Highway, Rahway, NJ 07065 (USA)

[g] J. Stellabott
Basic Pharmaceutical Sciences, Merck Research Laboratories
P.O. Box 4, Sumneytown Pike, West Point, PA 19486 (USA)

Supporting information for this article is available on the WWW under <http://dx.doi.org/10.1002/cmde.201200025>.

tinct but partially overlapping distributions in the CNS and project into regions of the brain that regulate arousal and the sleep/wake cycle. Orexin A binds with similar affinity to OX₁R and OX₂R, while orexin B binds more avidly to OX₂R.

There is strong genetic linkage between orexin hypofunction and regulation of wakefulness. Inbred dogs with inheritable loss-of-function mutations in OX₂R have a narcoleptic phenotype.^[7] Human narcolepsy is associated with a loss of orexin-producing neurons in the hypothalamus, with low to absent levels of orexins in cerebrospinal fluid (CSF).^[8] Significant dysregulation of the sleep/wake cycle is observed in genetically modified mice with loss of orexinergic neurons or deletion of the *prepro-orexin* gene.^[9] Secretion of orexin in the CNS occurs with circadian frequency; orexinergic neurons become more active during periods of wakefulness and become quiescent during sleep.^[10] When administered centrally, orexin peptides are sufficient to induce wakefulness and locomotor activity across species including mice, rats, dogs, and monkeys.^[11] As further validation of the role of orexins, small-molecule orexin antagonists dose-dependently promote sleep in rats, dogs, mice and humans.^[12]

Our laboratory recently described the discovery of suvorexant (**1**, MK-4305), a dual orexin receptor antagonist (DORA) currently in phase III clinical studies for the treatment of insomnia (Figure 1).^[13] Suvorexant has high affinity for both the OX₁ and

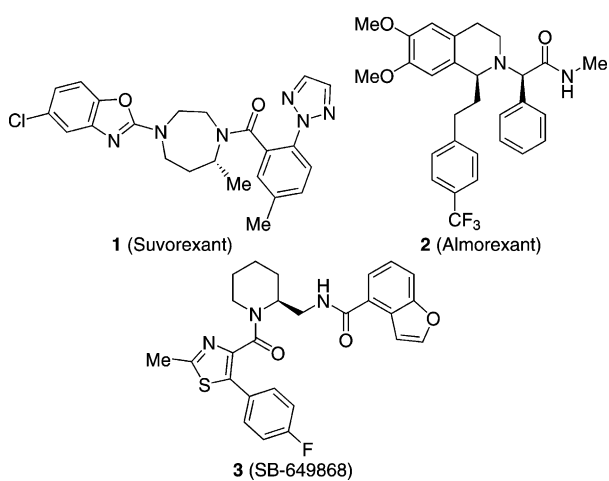


Figure 1. DORAs entering clinical studies.

OX_2 receptors and promotes sleep across multiple species, including humans. Indeed, clinical proof-of-concept studies have established that suvorexant dose-dependently increases sleep efficiency in patients with primary insomnia.^[14] Suvorexant is a member of the 1,4-diazepane-based structural class, a chemotype that we have previously described.^[15] Two structurally distinct DORAs, almorexant (**2**) and SB-649868 (**3**) have also entered clinical studies (Figure 1).

Almorexant (**2**) has been reported to decrease wakefulness in both rats and dogs, and first achieved

clinical proof of concept in treating symptoms of insomnia,^[16] although clinical development was subsequently halted. SB-649868 (3) was identified by GlaxoSmithKline as a potent DORA and entered clinical trials in 2005.^[17] Preclinically, SB-649868 was shown to be efficacious in rodent and primate sleep models;^[18] it was placed on clinical hold in late 2007 following phase II studies due to the emergence of reported pre-clinical toxicity.

Herein we describe the discovery of [(2R,5R)-5-{[(5-fluoropyridin-2-yl)oxy]methyl}-2-methylpiperidin-1-yl][5-methyl-2-(pyrimidin-2-yl)phenyl]methanone (MK-6096), a potent and reversible dual orexin receptor antagonist currently in clinical development for the treatment of primary insomnia.

Results and Discussion

The efforts described herein began with known piperidine carboxamide **4**.^[19] Newly synthesized compounds were evaluated in a radioligand displacement assay to measure binding affinity (expressed as K_i values) and subsequently assayed in a fluorimetric imaging plate reader (FLIPR) format, which provides a functional readout of receptor antagonism in CHO cells that overexpress human receptors (data reported as IC_{50} values). Orexin antagonist **4** possessed good potency with respect to OX₁R and OX₂R receptor binding. Despite excellent potency, DORA **4** had high plasma clearance in preclinical species and poor physicochemical properties. Our initial investigation probed the transposition of the α -substituent from the 2-position to the 3-position while maintaining a three-carbon-atom linkage between the piperidine nitrogen atom and the oxygen of the aryl ether to give compound **5** (Figure 2). This transposition resulted in a >40-fold loss in potency at both orexin receptor subtypes. Earlier work from this laboratory indicated the cyclic constraint found in the piperidine is not essential for good receptor potency.^[20] In fact, the unconstrained amidoproxy aryl ether **6** was only fourfold less potent with respect to OX₂R binding. Acyclic DORA **6** also exhibited high clearance in preclinical species and poor physicochemical properties. Our initial efforts focused on understanding why the α -substituted piperidine carboxamide **4** was preferred for high potency relative to the 3-substituted analogue **5**, given the results with the unconstrained linear carboxamide **6**.

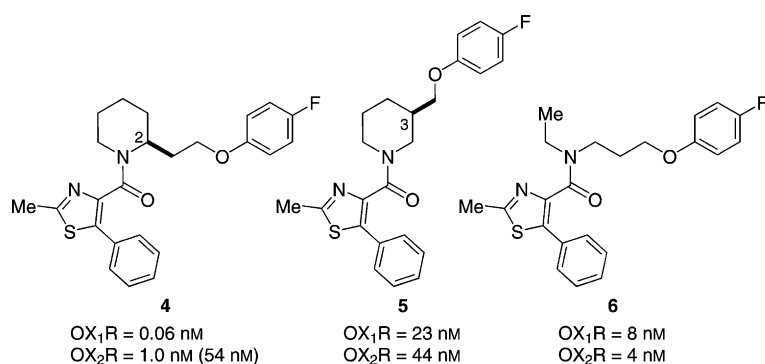


Figure 2. Constrained and unconstrained amidopropoxy ethers.

Minimization of 1,3-allylic strain governs the preferred conformations for 2-substituted piperidines when the nitrogen atom is sp^2 hybridized.^[21] In the case of compound **4**, the 2-substituent would be predicted to adopt a pseudo-axial orientation to minimize eclipsing interactions between the amide carbonyl and the 2-alkyl substitution.^[22] In contrast, the 3-substituted piperidine carboxamide would be predicted to have the 3-alkyl substitution oriented pseudo-equatorially in the lowest-energy ground state. Previously we reported conformational analyses of potent diazepane-based DORAs using single-crystal X-ray, molecular modeling, and ^1H NMR solution analyses, suggesting that diazepane DORAs prefer to adopt a U-shaped conformation both in solution and in the solid state.^[23] The conformational properties of these cyclic carboxamides can be complex, with multiple ring conformers present and restricted rotation around the $\text{N}-\text{C}=\text{O}$ bond of the amide. Additional studies with more highly constrained molecules have suggested that this U-shaped conformation, which is partly stabilized by a $\pi-\pi$ interaction, may represent a bioactive conformation for orexin receptor binding.^[24] Inspection of **4** reveals that the 2-substituted piperidine carboxamide might potentiate a similar $\pi-\pi$ interaction observed in the diazepane series and provide access to a bioactive conformation (Figure 3).

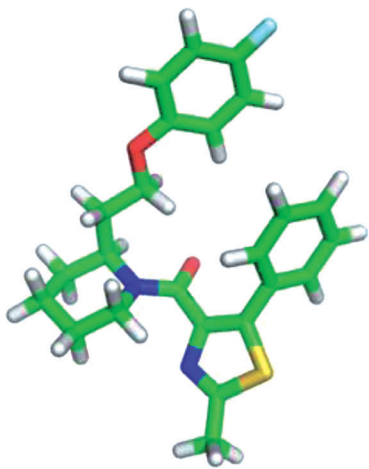
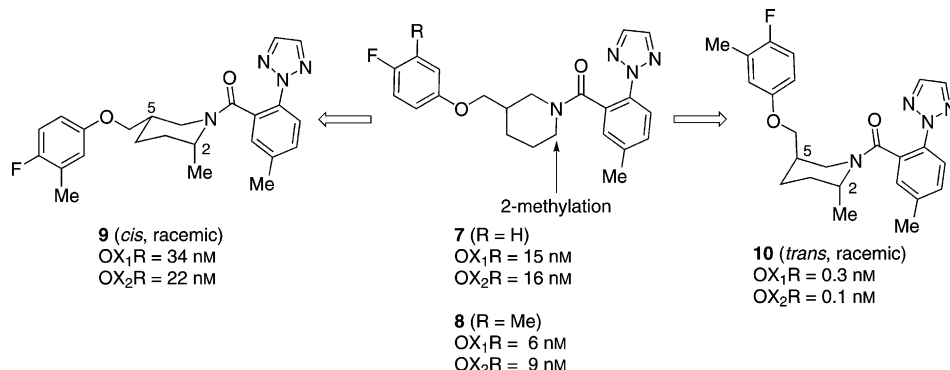


Figure 3. Predicted of low-energy conformation of compound **4**.

We explored a strategy to induce an axial orientation for the 3-alkyl substituent by installing a methyl group at either α -position adjacent to the sp^2 -hybridized nitrogen atom of the piperidine. In either case, 1,3-allylic strain should provide a bias for the axial orientation of the α -methyl substituent. Provided

that the (3)- CH_2OR substituent is oriented *trans* to the methyl substituent on the piperidine ring, it would be expected that the two substituents on the piperidine would be disposed in a *trans*-dixial orientation.

Installation of the methyl group in the two α -positions of the piperidine was performed on scaffold **5** (Schemes 1 and 3). Replacement of the phenylthiazole carboxamide with the tri-

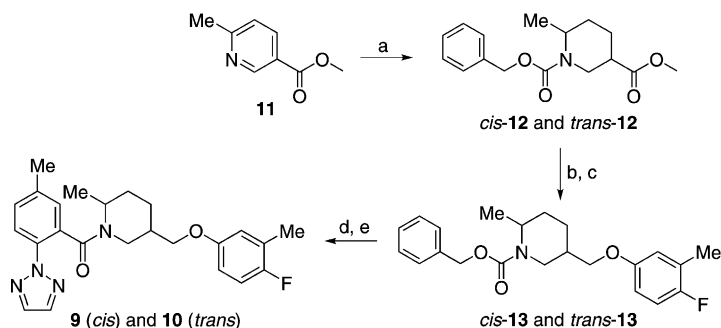


Scheme 1. α -Methylation on piperidine carboxamide **8**.

zoyl benzamide improved binding affinity for compound **7** versus **5**.^[25] A further enhancement in potency was realized by replacing the 4-fluorophenyl ether with a 3-methyl-4-fluorophenyl ether to provide **8**. Insertion of a 2-methyl group on **8** provided *cis* isomers **9** and *trans* isomers **10**. The racemic *trans* isomers were exceptionally potent, gaining 20- and 90-fold in OX_1R and OX_2R binding affinities, respectively, over the unsubstituted **8**. In contrast, the *cis* isomers **9** were less potent than **8**. While we anticipated the α -methylation might increase the binding affinity of **8** by directing the 5-substituent in an axial orientation, the magnitude of this effect on receptor potency was remarkable.

The 2,5-disubstituted piperidine derivatives were synthesized as shown in Scheme 2. Hydrogenation of 6-methyl nicotinate **11** by using platinum oxide in acetic acid under moderate pressure afforded a mixture of *cis/trans* piperidines in a 4.5:1 ratio. The carboxylate esters **12** were separable, and both were independently advanced through the subsequent synthetic sequence. Reduction of the ester followed by formation of the aryl ether through a Mitsunobu reaction provided aryl ether **13**. Hydrogenolysis of the benzyl carbamate **13** followed by amide formation with 2-(2*H*-1,2,3-triazol-2-yl)-5-methylbenzoic acid^[26] provided orexin antagonists **9** and **10**.

Additional SAR development was carried out on piperidine **10**. The objective was to improve physicochemical properties while maintaining good receptor potency. For compounds in this series, high lipophilicity correlated with high intrinsic clearance in human and animal liver microsomes and poor preclinical pharmacokinetics. Heterocyclic replacements for the 3-methyl-4-fluorophenyl ether were investigated (Table 1). Replacing the phenyl ether with aza-heterocycles such as 1,5-naphthyridine **14**, pyrimidine **15**, or pyrazine **16** was not tolerated. Although replacing the phenyl ether with a 2-pyridine **17**



Scheme 2. Synthesis of 2,5-disubstituted piperidine DORAs. *Reagents and conditions:* a) H_2 (g), PtO_2 , AcOH then CBz-Cl , Et_3N , 64% *cis*-12 and 14% *trans*-12; b) LiAlH_4 , THF ; c) 3-methyl-4-fluorophenol, $\text{Ph}_3\text{P-PS}$, DIAD ; d) Pd(OH)_2 , H_2 (g), EtOH ; e) 5-methyl-2-(2H-1,2,3-triazol-2-yl)benzoic acid, EDC , HOBT , Et_3N .

Table 1. SAR exploration on the aryl ether. ^[a]				
R	Compd	K_i [nM] OX_1R	K_i [nM] OX_2R	clog P (measured)
	10	0.3	0.1	4.64 (>3.54)
	14	58	98	3.88
	15	340	55	2.57
	16	58	7	3.44
	17	11	4	3.37
	18	1.0	0.2	3.53 (2.57)

[a] Values are the mean of two or more experiments.

attenuated receptor potency, binding affinity could be regained by reinstallation of the *para*-fluoro substituent on pyridine **18**. Importantly, the incorporation of the pyridine significantly improved the physicochemical properties of **18** versus **10**, decreasing measured $\log P$ from >3.5 to 2.7.

To this point, optimization in the piperidine series had primarily focused on 2,5-disubstitution. As an alternate strategy for inducing a *trans*-diaxial substitution pattern on the piperidine carboxamide, we could also install a methyl group in the alternate α -position. The 2-methyl-3-alkylpiperidine derivatives were

prepared from the commercially available 2,3-substituted piperidine **19** (Scheme 3).

As shown in Table 2, the 2,3-*trans*-disubstituted piperidine **21** also gained significant potency versus the non-methylated piperidine **22**, although the extent of this gain in potency on OX_2R was less than that observed with 6-methyl substitution for compound **18**. This observation is consistent with our structural hypothesis that α -methylation favors the *trans*-diaxially substituted piperidine with axial orientation for the 3- CH_2OAr group. There were no specific advantages of the 2,3- versus 2,5-disubstitution, so further SAR exploration centered on compound **18**.

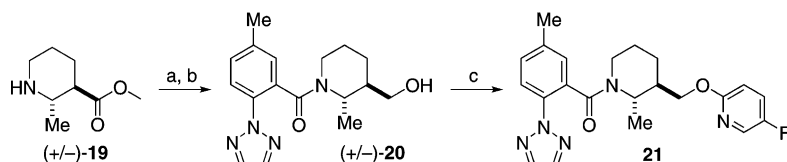
Although compound **18** had exceptional potency, it suffered from poor aqueous solubility (<

Table 2. The effect of α -methylation on piperidine potency.

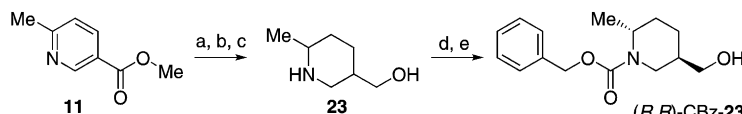
Compd	R^1	R^2	K_i [nM] OX_1R	K_i [nM] OX_2R
22	H	H	96	29
18	Me	H	1.0	0.2
21	H	Me	0.19	4.3

$10 \mu\text{g mL}^{-1}$) and low oral bioavailability in rats (<10%). Further optimization focused on the aryl moiety of the carboxamide. For key molecules listed in this table, the synthetic sequence was optimized to provide improved access to the *R,R-trans*-2,5-disubstituted piperidine (Scheme 4). Hydrogenation of pyridine **11** provided a ~4:1 ratio of racemic *cis/trans* piperidines. This mixture could be equilibrated by treatment with sodium methoxide in methanol at 50°C for four days. After equilibration, the ratio of *cis/trans* inverted, favoring the thermodynamically more stable *trans* isomer in a 4:1 ratio. The unpurified product from this isomerization was reduced, and the crude amino alcohol **23** was protected as a carbamate. The adduct from this reaction was then purified by HPLC on a chiral stationary support to provide pure (*R,R*)-CBz-**23** in high enantiomeric excess.

Replacement of the triazoyl moiety present in **18** with a phenyl group (compound **24**) improved receptor binding potency, but compromised physicochemical properties (aqueous solubility: $8 \mu\text{g mL}^{-1}$). Compounds such as **24** with higher lipo-



Scheme 3. Preparation of the 2,3-disubstituted piperidine carboxamide DORAs. *Reagents and conditions:* a) LIAH_4 , THF ; b) 5-methyl-2-(2H-1,2,3-triazol-2-yl)benzoyl chloride, CH_2Cl_2 , 55% for two steps; c) 5-fluoropyridin-2-ol, Ph_3P , DIAD , chiral HPLC, 77%.



Scheme 4. Optimized synthesis of (R,R)-trans-disubstituted piperidine. *Reagents and conditions:* a) PtO₂, H₂(g), AcOH; b) NaOMe, MeOH, 50 °C, 4 days; c) LiAlH₄, THF, 0 °C; d) CBz-Cl, Et₃N, CH₂Cl₂; e) Chiracel OD, 16% overall.

philicity tended to have more highly shifted IC₅₀ values in the FLIPR assay (Table 3). The triazolyl substituent in **18** could be replaced with a pyrazole **25**, pyridine **26**, or pyrimidine **27**. In the case of the pyrazole **25**, significant OX₁R activity was lost. Pyridyl **26** improved the physicochemical properties with a modest decrease in potency. The pyrimidinyl substituent in **28** afforded the best balance between OX₁R/OX₂R potency and provided an unexpected improvement in aqueous solubility. The pyrimidine substitution also drove an increase in the plasma-free fraction. Orexin antagonists with higher free fractions generally achieved higher CSF concentrations and greater sleep-promoting efficacy at comparably lower plasma levels.^[27] The 5-tolylmethyl substituent in **28** was critical for potency; deletion of this methyl group or replacement with a fluorine (compound **27**) compromises OX₁R potency.

Analogue **28** emerged as the most interesting molecule from these SAR studies. Low-temperature ¹H NMR studies indicated an equilibrating mixture of four isomers at a 74:16:7:3

ratio. The two most abundant isomers both have the piperidine in a chair conformation with *trans*-dialixal substitution, but differ in having slow rotation around the amide N—C=O bond. The major isomer (74%) is depicted in Figure 4, with strong NOEs observed between the protons on the two aryl moieties. This preferred conformation was confirmed in the solid state with a single-crystal X-ray of **28**.^[28] However, in the solid state, the preferred conformation is the isomer with the diarylamide substituent rotated into the configuration where the pyrimidine ring is adjacent to the fluoropyridine group. The X-ray structure of **28** shows the *trans*-dialixal arrangement of the 2,5-disubstituted piperidine.

Orexin receptors are conserved across species, and com-

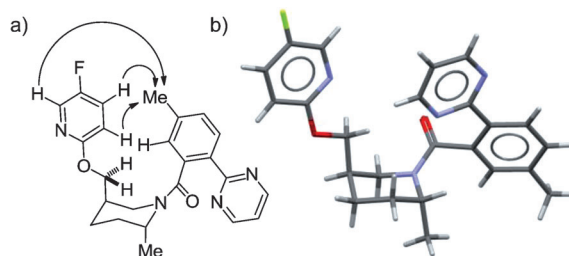


Figure 4. a) ¹H NMR NOEs observed for compound **28** and b) X-ray crystal structure of **28**.

Table 3. Optimization of the biaryl carboxamide.^[a]

R	Compd	K_i [nM] ^[b] OX ₁ R	K_i [nM] ^[b] OX ₂ R	HP [%] ^[d]	Sol. [μ M] ^[e]
	18	1.0 (14)	0.2 (10)	97.8	< 10
	24	0.7 (48)	0.1 (58)	> 99	< 10
	25	250 (47)	0.7 (11)	99.1	NA
	26	3.2 (28)	0.4 (13)	97.9	NA
	27	10 (32)	0.6 (10)	96	174
	28	2.5 (11)	0.3 (11)	94.1	192

[a] Values are the mean of two more experiments. [b] K_i of binding. [c] Determined by FLIPR assay. [d] Human plasma protein binding. [e] Solubility: measured at pH 7 by high-throughput solubility assay.

pound **28** is highly potent in human, rat, dog, mouse, rabbit, and rhesus in vitro orexin binding assays.^[29] Compound **28** has a favorable pharmacokinetic profile in preclinical species. The pharmacokinetics of **28** were evaluated in Sprague–Dawley rats and beagles (Table 4). After i.v. administration, **28** exhibited high plasma clearance in rats and low to moderate plasma clearance in dogs (Table 4). The terminal half-life is short in both species, ranging from 0.5 to 2.3 h. The bioavailability for **28** was 25 and 26% in rats and dogs, respectively, with peak plasma concentrations in both species achieved rapidly after oral dosing. Plasma protein binding for **28** was high with measured values of 94.8, 94.2, and 97.5% in rat, dog, and human, respectively. The major route of clearance for **28** in preclinical species was via oxidative metabolism with significant oxidation

Table 4. Pharmacokinetics of compound **28** in rat and dog.

Species	Dose [mg kg ⁻¹]	CL [mL min ⁻¹ kg ⁻¹]	V _{dss} [L kg ⁻¹]	t _{1/2} [h]	p.o. ^[a]			
					Dose [mg kg ⁻¹]	AUC [μM h]	C _{max} [μM]	t _{max} [h]
rat	2	67	1.6	0.5	15	2.3	1.9	0.4
dog	0.5	5.8	1.0	2.3	3	4.6	1.8	0.4

[a] 20% aqueous D- α -tocopheryl poly(ethylene glycol) succinate; values are the means of $n=3$ experiments.

of the benzylic carbon observed. The rate of liver microsomal metabolism for **28** in human was closer to that in dog and lower than that in rat. The microsomal intrinsic clearance ($CL_{int,mic}$) is $33\text{--}82\text{ mL min}^{-1}(\text{mg protein})^{-1}$ in dog and human, while in rat, $CL_{int,mic}$ is $\sim 390\text{ mL min}^{-1}(\text{mg protein})^{-1}$. Compound **28** is not a potent reversible inhibitor of CYP3A4, 2C9, or 2D6 (IC_{50} values: 35, 55, and $>100\text{ μM}$, respectively). It is also not a potent time-dependent inhibitor of CYP3A4, with respective k_{inact} and K_i values of 0.12 min^{-1} and 17 μM .

DORA **28** dose-dependently promotes sleep in rats and dogs following oral administration, and decreases locomotor activity in rats relative to vehicle treatment in seven-day cross-over studies.^[29] When dosed in the active phase to rats at 3 and 10 mg kg^{-1} p.o., DORA **28** elicited dose-dependent decreases in active wake (-30.8 to -49.2%) and concomitant increases in both REM ($+28.9$ to 48.4%) and non-REM sleep (9.9 to 21%). In dog EEG-telemetry studies, **28** promoted sleep at oral doses of 0.25 and 0.5 mg kg^{-1} when dosed in the active phase. At these doses, significant changes in sleep measures were recorded (Table 5).

Table 5. Dose-dependent sleep changes in male beagle dogs with compound **28**.^[a]

Dose [mg kg ⁻¹]	Active wake [%]		Sleep [%]		REM [%]
			Slow wave I	Slow wave II	
0.25	-16.9^*		$+15.3$	$+88.8$	$+70.7$
0.5	-22.7^*		$+39.7$	$+371.3^{**}$	$+133.6$

[a] Quantitation of sleep stage duration expressed as mean percent change relative to treatment with vehicle alone in the 3 h following MK-6096 treatment (* $p < 0.05$, ** $p < 0.01$, population t-test).

Dog pharmacokinetics were assessed in a cohort of satellite animals. At effective doses of 0.25 and 0.5 mg kg^{-1} , oral administration of **28** was associated with C_{max} values of 0.19 and 0.47 μM , respectively, corresponding to $AUC_{0-24\text{ h}}$ values of 0.38 and 1.3 μM h . No attenuation in the response to drug was observed over 5–7 days of cumulative dosing in either rats or dogs.

Preclinical data suggest that **28** has high potential for brain penetration in humans. Compound **28** is not a substrate for human or rat P-glycoprotein (P-gp)-mediated efflux in the P-gp-expressing LLC-PK-1 cell line, and has high passive permeability in control LLC-PK1 cells ($P_{app}=29\times 10^{-6}\text{ cm s}^{-1}$). Based on these preclinical data, **28** was projected to have good brain penetration and a favorable human PK profile with a predicted $t_{1/2}=1\text{--}6\text{ h}$ and rapid absorption following oral administration,

consistent with the desired profile for a sedative-hypnotic. Compound **28** has favorable physicochemical properties as a neutral crystalline form (mp: 134.8°C) with $M_r=420\text{ Da}$, polar surface area of 61 Å ,^[2] and good solubility in simulated intestinal fluid (fasted state; 0.11 mg mL^{-1}).

DORA **28** also has high selectivity for orexin receptor binding. Evaluation of **28** in a counter-screen panel of 170 receptor and enzyme targets revealed no ancillary activities with IC_{50} values $<10\text{ μM}$. Compound **28** is not a potent inhibitor of the hERG channel^[30] with $IC_{50}=46\text{ μM}$, and no treatment-related cardiovascular changes were observed in preclinical evaluations of this compound in an anesthetized, vagotomized dog model at plasma concentrations up to 18 μM .^[31]

Compound **28** achieves high receptor occupancy in a humanized OX₂R-overexpressing transgenic rat brain assay. Following i.v. infusion to anesthetized rats, **28** achieved 90% occupancy with a plasma exposure of 142 nM .^[32] Binding of OX₂R by **28** is fully reversible as demonstrated by in vitro kinetic displacement assays. Based on these favorable preclinical data, **28** was selected to move into clinical studies and designated as MK-6096. MK-6096 has recently advanced into phase II clinical studies for the treatment of insomnia.^[33]

Conclusions

In summary, we have identified a dual orexin receptor antagonist, MK-6096, with excellent in vitro potency, brain penetration, physicochemical properties, selectivity, and pharmacological activity across multiple preclinical species. We previously described the discovery and characterization of suvorexant, a DORA currently in late-stage clinical studies. With respect to preclinical efficacy, MK-6096 is more potent than suvorexant in rat and dog EEG studies. Furthermore, the measured receptor occupancies for MK-6096 versus suvorexant in transgenic rats overexpressing human OX₂R (Occ_{90} values = 0.142 and 1.1 μM , respectively) suggest greater potency for MK-6096. The design of MK-6096 was driven in part by an understanding of the conformational properties anticipated to be favorable for high orexin receptor activity. Earlier conformational studies on diazepane carboxamides provided a strong rationale for designing molecules with a central template that permitted intramolecular aryl–aryl interactions. In particular, piperidine methylation adjacent to the amide nitrogen atom provided analogues with 2,5-trans-diaxial substitution and enabled a critical π – π interaction. MK-6096 represents a novel therapy for treating insomnia and other disorders related to sleep/wake dysregulation.

Experimental Section

Biology

All animal studies were performed according to the NIH Guide for the Care and Use of Laboratory Animals, and experimental protocols were reviewed by the Merck Animal Care and Use Committee. Protocols for the radioligand binding, FLIPR, and receptor occupancy assays as well as polysomnographic analysis in rats and dogs have been previously disclosed.^[13,29]

Chemistry

All solvents used were commercially available “anhydrous” grade, and reagents were used without purification unless otherwise noted. Non-aqueous reactions were carried out in oven- or heat-gun-dried glassware under a N_{2(g)} atmosphere. Magnetic stirring was used to agitate the reactions and they were monitored for completion by either TLC (silica gel 60, Merck) or LC–MS. A Smith-Creator microwave from Personal Chemistry was used for microwave heating, and a CombiFlash system using RediSep cartridges by Teledyne Isco was used for silica gel chromatography with fraction collection at λ 254 nm. Reversed-phase HPLC purification was carried out on a Waters HPLC (XBridge Prep C₁₈ 5 μ m 19 \times 150 mm column) using a gradient of 0.1% TFA in H₂O/CH₃CN with sample collection triggered by photodiode array detection. The reported yields are for isolated compounds of $\geq 95\%$ purity, unless otherwise noted, and were not extensively optimized. Purity analysis was carried out by HPLC with a Waters 2690 Separations Module equipped with a YMC Pro 50 \times 3 mm i.d. C₁₈ column interfaced with a Waters Micromass ZMD spectrometer using a gradient of 0.05% TFA in H₂O/CH₃CN with UV detection at λ 215 and 254 nm. ¹H and ¹³C NMR spectra were recorded on a Varian INOVA 400, 500, or 600 MHz spectrometer, and all chemical shifts are referenced to an internal standard of tetramethylsilane or the CDCl₃ solvent peak, respectively. High resolving power accurate mass measurement electrospray (ES) and atmospheric pressure chemical ionization (APCI) mass spectral data were acquired by use of a Bruker Daltonics 7T Fourier transform ion cyclotron resonance mass spectrometer (FT-ICR MS). Optical rotations were determined at 23 °C on a PerkinElmer 241 spectrometer in the solvents and at the concentrations specified.

The substituted piperidine orexin receptor antagonists described in this manuscript exhibit complex conformations in solution, and exist in multiple conformations as a result of hindered rotations that are slow on the NMR timescale. The proton spectra of compounds 5, 9, 10, 13, 14, 15, 16, 17, 18, 20, 21, 24, 25, 26, 27, 29, and 30 consist of broad, overlapping multiplets precluding a detailed coupling constant analysis, and we feel that pictorial reproductions of the NMR spectra are more informative for comparative purposes; thus, NMR resonances of final compounds will not be listed in numerical format. Instead, we include reproductions of the ¹H and ¹³C NMR spectra at 25 °C of all final compounds in the Supporting Information. For compound 28 only, ¹H and ¹³C chemical shifts were assigned from the analysis of COSY, HSQC, and HMBC spectra acquired on a sample dissolved in CDCl₃ at 25 °C.

[3-(Hydroxymethyl)piperidin-1-yl](2-methyl-5-phenyl-1,3-thiazol-4-yl)methanone: A solution of 2-methyl-5-phenyl-1,3-thiazole-4-carboxylic acid (381 mg, 1.74 mmol), piperidin-3-ylmethanol (200 mg, 1.74 mmol), EDC (399 mg, 2.08 mmol), HOBT (282 mg, 2.08 mmol), and Et₃N (0.847 mL, 6.08 mmol) in DMF (5 mL) in a microwave vessel was sealed and heated at 150 °C in a microwave reactor for 10 min. The mixture was diluted with EtOAc and washed

with saturated aqueous NaHCO₃, H₂O, and brine. The organic layer was dried over Na₂SO₄, filtered, and concentrated. The crude material was purified by gradient elution on silica gel [0 \rightarrow 10% EtOH/NH₄OH/H₂O 10:1:1 in EtOAc] to yield the product as a colorless film (228 mg, 42%). Please see figures at the end of the Supporting Information for reproductions of 500 MHz ¹H and 100.5 MHz ¹³C NMR spectra in CDCl₃ at 25 °C. LRMS = 317.1 [M+H].

{3-[(4-Fluorophenoxy)methyl]piperidin-1-yl}(2-methyl-5-phenyl-1,3-thiazol-4-yl)methanone 5: A cooled solution (0 °C) of [3-(hydroxymethyl)piperidin-1-yl](2-methyl-5-phenyl-1,3-thiazol-4-yl)methanone (228 mg, 0.72 mmol), 4-fluorophenol (81 mg, 0.72 mmol), and Ph₃P (189 mg, 0.72 mmol) was treated dropwise with diethyl azodicarboxylate (0.113 mL, 0.72 mmol). After stirring overnight at room temperature, the mixture was concentrated. The residue was absorbed onto silica gel and purified by gradient elution on silica gel (0 \rightarrow 100% EtOAc in hexanes) to yield 5 as a pale-yellow solid (52 mg, 18%). Please see figures at the end of the Supporting Information for reproductions of 500 MHz ¹H and 100.5 MHz ¹³C NMR spectra in CDCl₃ at 25 °C. IR (KBr): ν = 2927, 2858, 1634, 1505, 1208, 827, 757 cm⁻¹; HRMS calcd for C₂₃H₂₃FN₂O₂S [M+H]: 411.1538, found: 411.1526.

Synthesis of 9 and 10: (+/-)-1-benzyl 3-methyl-6-methylpiperidine-1,3-dicarboxylate cis-12 and trans-12: A solution of methyl 6-methylpyridine-3-carboxylate (1.1 g, 7.28 mmol) in EtOH (25 mL) was treated with platinum(IV) oxide (0.165 g, 0.728 mmol) and acetic acid (0.417 mL, 7.28 mmol). A Parr bottle was evacuated and backfilled with H_{2(g)} three times and stirred under a H_{2(g)} atmosphere (45 atm) at room temperature overnight. The mixture was filtered through Celite, and the filter cake was washed with MeOH. The filtrate was treated with TEA (4.06 mL, 29.1 mmol) and CBz-Cl (1.143 mL, 8.00 mmol). The mixture was stirred at room temperature for 30 min and concentrated. The residue was partitioned between EtOAc and H₂O. The organic phase was dried over Na₂SO₄, filtered and concentrated. The crude material was purified by gradient elution on silica gel (0 \rightarrow 25% EtOAc in hexanes) to yield cis-12 as a colorless oil (1.36 g, 64%) and trans-12 as a colorless oil (0.303 g, 14% yield). Please see figures at the end of the Supporting Information for reproductions of 500 MHz ¹H and 100.5 MHz ¹³C NMR spectra in CDCl₃ at 25 °C. LRMS = 292.1 [M+H].

(+/-)Benzyl-5-[(4-fluoro-3-methylphenoxy)methyl]-2-methylpiperidine-1-carboxylate; (cis)-13: A solution of cis-12 (300 mg, 1.030 mmol) in THF (10 mL) was cooled to -78 °C and treated slowly with LiAlH₄ (1.119 mL, 2.57 mmol). The solution was warmed to 0 °C and stirred for 20 min, then treated dropwise with 0.1 mL H₂O, 0.1 mL 15% NaOH, and 0.3 mL H₂O successively. Na₂SO₄ was added to the mixture. After stirring overnight at room temperature, the mixture was filtered through a pad of Celite, and the filtrate was concentrated to yield alcohol product cis-13, which was taken on crude into the next step. A solution of the crude alcohol (270 mg, 1.025 mmol), 3-methyl-4-fluorophenol (155 mg, 1.230 mmol), and Ph₃P-resin bound (572 mg, 1.230 mmol, 2.15 mmol g⁻¹) in CH₂Cl₂ (3 mL) was treated with diisopropyl azodicarboxylate (DIAD; 0.239 mL, 1.230 mmol). The mixture was stirred overnight, filtered, and the filtrate was concentrated. The crude material was purified by gradient elution on silica gel (0 \rightarrow 25% EtOAc in hexanes) to yield cis-13 as a yellow oil (228 mg, 60% yield) over two steps. Please see figures at the end of the Supporting Information for reproductions of 500 MHz ¹H and 100.5 MHz ¹³C NMR spectra in CDCl₃ at 25 °C. LRMS = 372.1 [M+H].

(+/-)cis-{5-[(4-Fluoro-3-methylphenoxy)methyl]-2-methylpiperidin-1-yl}[5-methyl-2-(2H-1,2,3-triazol-2-yl)phenyl]methanone (9):

A solution of *cis*-**13** (228 mg, 0.614 mmol) in EtOH (5 mL) was treated with Pd(OH)₂ on carbon (43.1 mg, 0.061 mmol). The flask was evacuated and backfilled with H_{2(g)} three times and stirred under a H_{2(g)} atmosphere (1 atm) at room temperature for 30 min. The mixture was filtered through a syringe filter. The filtrate was concentrated to yield an amine product which was taken on crude into the next step. A solution of the crude amine (146 mg, 0.615 mmol) in DMF (4 mL) was treated with 5-methyl-2-(2H-1,2,3-triazol-2-yl)benzoic acid (125 mg, 0.615 mmol), EDC (142 mg, 0.738 mmol), HOBT (113 mg, 0.738 mmol), and TEA (0.257 mL, 1.846 mmol). After stirring at room temperature overnight, the mixture was diluted with EtOAc, washed with H₂O (3×) and once with brine. The organic phase was dried over Na₂SO₄, filtered, and concentrated. This material was purified by gradient elution RP HPLC [5→95% CH₃CN in H₂O (0.1% TFA)] to give pure fractions which were concentrated, diluted with EtOAc, and washed with saturated aqueous NaHCO₃. The organic phase was dried over Na₂SO₄, filtered, and concentrated to yield **9** as a white solid (149 mg, 57% yield) over two steps. Please see figures at the end of the Supporting Information for reproductions of 500 MHz ¹H and 100.5 MHz ¹³C NMR spectra in CDCl₃ at 25 °C. IR (KBr): ν =2929, 2862, 1629, 1499, 1436, 1410, 1202, 951, 823, 731 cm⁻¹; HRMS calcd for C₂₄H₂₇FN₄O₂ [M+H]: 423.2191, found: 423.2193.

(+/-)Benzyl-5-[{(4-fluoro-3-methylphenoxy)methyl]-2-methylpiperidine-1-carboxylate (*trans*-13**):** A solution of *trans*-**12** (300 mg, 1.030 mmol) in THF (10 mL) was cooled to -78 °C and treated slowly with LiAlH₄ (1.119 mL, 2.57 mmol). The solution was warmed to 0 °C and stirred for 20 min, then treated dropwise with 0.1 mL H₂O, 0.1 mL 15% NaOH, and 0.3 mL H₂O successively. Na₂SO₄ was added to the mixture. After stirring overnight at room temperature, the mixture was filtered through a pad of Celite, and the filtrate was concentrated to yield the alcohol product which was taken on crude into the next step. A solution of the crude alcohol (270 mg, 1.025 mmol), 3-methyl-4-fluorophenol (155 mg, 1.230 mmol), and resin-bound Ph₃P (572 mg, 1.230 mmol, 2.15 mmol g⁻¹) in CH₂Cl₂ (3 mL) was treated with DIAD (0.239 mL, 1.230 mmol). The mixture was stirred overnight, filtered, and the filtrate was concentrated. The crude material was purified by gradient elution on silica gel (0→25% EtOAc in hexanes) to yield *trans*-**13** as an orange oil (103 mg, 27%) over two steps. Please see figures at the end of the Supporting Information for reproductions of 500 MHz ¹H and 100.5 MHz ¹³C NMR spectra in CDCl₃ at 25 °C. LRMS=372.1 [M+H].

(+/-)*trans*-{5-[(4-Fluoro-3-methylphenoxy)methyl]-2-methylpiperidin-1-yl}[5-methyl-2-(2H-1,2,3-triazol-2-yl)phenyl]methanone (10**):** A solution of *trans*-**13** (100 mg, 0.269 mmol) in EtOH (5 mL) was treated with Pd(OH)₂ (18.90 mg, 0.027 mmol). The flask was evacuated and backfilled with H_{2(g)} three times and stirred under a H_{2(g)} atmosphere (1 atm) at room temperature for 30 min. The mixture was filtered through a syringe filter. The filtrate was concentrated to yield amine product which was taken on crude into the next step. A solution of the crude amine (64 mg, 0.270 mmol) in DMF (4 mL) was treated with 5-methyl-2-(2H-1,2,3-triazol-2-yl)benzoic acid (54.8 mg, 0.270 mmol), EDC (62.0 mg, 0.324 mmol), HOBT (49.6 mg, 0.324 mmol), and TEA (0.113 mL, 0.809 mmol). After stirring at room temperature overnight, the mixture was diluted with EtOAc, washed with H₂O (3×), and once with brine. The organic phase was dried over Na₂SO₄, filtered, and concentrated, diluted with EtOAc, and washed with saturated aqueous NaHCO₃. The organic phase was dried over Na₂SO₄, filtered, and concentrat-

ed to yield **10** as a white solid (53 mg, 47%) over two steps. Please see figures at the end of the Supporting Information for reproductions of 500 MHz ¹H and 100.5 MHz ¹³C NMR spectra in CDCl₃ at 25 °C. IR (KBr): ν =2934, 2868, 1634, 1501, 1434, 1204, 1033, 962, 834, 765 cm⁻¹; HRMS calcd for C₂₄H₂₇FN₄O₂ [M+H]: 423.2191, found: 423.2193.

(+/-)[3-(Hydroxymethyl)-2-methylpiperidin-1-yl][5-methyl-2-(2H-1,2,3-triazol-2-yl)phenyl]methanone (20**):** (2S,3R)-2-Methylpiperidine-3-carboxylic acid hydrochloride (**19**; 590 mg, 2.84 mmol) was dissolved in THF (14 mL) and cooled to 0 °C. To the stirring solution was added LiAlH₄ in THF (9.942 mL, 9.94 mmol) dropwise. The solution was allowed to stir at room temperature for 2 h. The reaction mixture was cooled to 0 °C. To the cooled solution was added successively 378 μ L H₂O dropwise, 378 μ L 15% NaOH solution, and 1.2 mL H₂O at once. The resulting biphasic mixture was stirred, and then Na₂SO₄ was added and stirred for an additional 30 min. The mixture was filtered through Celite, and the Celite cake was washed with MeOH/CH₂Cl₂, and concentrated to yield crude amino alcohol as an off-white solid, which was used in the next step as is.

The crude amino alcohol (330 mg, 2.55 mmol) was dissolved in CH₂Cl₂ (~7 mL) and then Et₃N (890 μ L, 6.39 mmol) was added and stirred. In a separate flask 5-methyl-2-(2H-1,2,3-triazol-2-yl)benzoyl chloride (623 mg, 2.81 mmol) was dissolved in CH₂Cl₂ (~7 mL), the solution was cooled to 0 °C. After 10 min, the solution containing the amino alcohol was added in small portions and upon complete addition, the ice bath was removed. The reaction was allowed to stir for 18 h. The reaction mixture was diluted with CH₂Cl₂, and then washed with saturated NaHCO₃ solution and brine, dried (Na₂SO₄), and concentrated. The residue was purified by silica gel chromatography (40 g) eluting with 0→50% EtOAc/hexanes. Pure fractions of desired product were concentrated to yield **20** as a white solid (440 mg, 55%). Please see figures at the end of the Supporting Information for reproductions of 500 MHz ¹H and 100.5 MHz ¹³C NMR spectra in CDCl₃ at 25 °C; LRMS=315.5 [M+H].

[(2S,3R)-3-[(5-Fluoropyridin-2-yl)oxy]methyl]-2-methylpiperidin-1-yl][5-methyl-2-(2H-1,2,3-triazol-2-yl)phenyl]methanone (21**):** Compound **20** (200 mg, 0.636 mmol) was dissolved in CH₂Cl₂. 5-Fluoropyridin-2-ol (90 mg, 0.795 mmol) and Ph₃P (334 mg, 1.272 mmol) were added, and the solution was stirred for 10 min. DIAD (186 μ L, 0.954 mmol) was added dropwise, and the solution was stirred for 1 h. The reaction mixture was diluted in EtOAc, washed with saturated NaHCO₃ brine, dried, and concentrated. The residue was purified on silica gel (40 g) eluting with 0→75% EtOAc/hexanes to yield a residue which was resolved by chiral SFC: Column AS-H, 4.6 mm×250 mm; eluting with 15% EtOH, 85% CO₂, 0.1% DEA at a flow rate of 2.4 mL min⁻¹ to yield 80 mg (32%) *rac*-**21** as a white solid. Compound **21** elutes first with t_R=3.78 min (25 mg, 10%). Please see figures at the end of the Supporting Information for reproductions of 500 MHz ¹H and 100.5 MHz ¹³C NMR spectra in CDCl₃ at 25 °C. $[\alpha]_D=+31.28$ (c=1.49, CHCl₃); IR (KBr): ν =2941, 1634, 1486, 1377, 1268, 1225, 1024, 952, 825 cm⁻¹; HRMS calcd for C₂₂H₂₄FN₅O₂ [M+H]: 410.1987, found: 410.1983.

Benzyl (2*R*,5*R*)-5-(hydroxymethyl)-2-methylpiperidine-1-carboxylate (2*R*,5*R*-CBz-23**):** A solution of the methyl 6-methylpyridine-3-carboxylate hydrochloride (23 g, 152 mmol) in EtOH (200 mL) was treated with 5 mol% PtO₂ (1.728 g, 7.61 mmol) and AcOH (8.71 mL, 152 mmol). A Parr bottle was evacuated and backfilled with H_{2(g)} three times and stirred under a H_{2(g)} atmosphere (310 kPa, recharged four times) at room temperature for 3 h. The mixture was

filtered through Celite, and the filter cake was washed with MeOH. The filtrate was concentrated to yield product with a ~3.5:1 *cis/trans* ratio. This material was diluted with MeOH (300 mL), treated with NaOMe (32.9 g, 183 mmol), heated at 50 °C, and stirred at this temperature for four days. The mixture was cooled to room temperature, neutralized to pH 7 with concentrated HCl, filtered through Celite and the filtrate was concentrated. The residue was suspended in MeOH and filtered again. The resulting filtrate was concentrated to yield 24 g of crude amine hydrochloride (~4:1 *trans/cis*).

A suspension of the amine hydrochloride, ~4:1 *trans/cis* (24 g, 124 mmol) in THF (900 mL) with overhead stirring was cooled to 0 °C and treated dropwise with LiAlH₄ (315 mL, 315 mmol) via addition funnel. After stirring for 30 min, maintaining at 0 °C, the mixture was treated dropwise via addition funnel with 14.4 mL H₂O, 14.4 mL 15% NaOH, and 43.2 mL H₂O successively. Na₂SO₄ was added to the mixture. After being stirred for 2 h at room temperature, the mixture was filtered, and the filtrate was concentrated to yield 15.3 g of crude amino alcohol. A solution of the crude amino alcohol (15.3 g, 118 mmol) in CH₂Cl₂ (200 mL) was treated with TEA (33.0 mL, 237 mmol), and CBz-Cl (18.60 mL, 130 mmol). The mixture was stirred at room temperature overnight and then concentrated. The residue was partitioned between EtOAc and H₂O. The organic phase was dried over Na₂SO₄, filtered, and concentrated. The crude material was purified by gradient elution on silica gel (0→100% EtOAc in hexanes) to yield 17.9 g racemic material (2.5:1 *trans/cis*). The *trans* material was separated away from the *cis* diastereomers, and the enantiomers resolved on a 10 cm o.d. Chiracel column by isocratic elution (87:13 hexanes/iPrOH) to yield 2*R*,5*R*-CBz-**23** as a tan oil (first eluting peak; 5.0 g, 16%) over three steps including the chiral separation (>99% ee). Please see figures at the end of the Supporting Information for reproductions of 500 MHz ¹H and 100.5 MHz ¹³C NMR spectra in CDCl₃ at 25 °C. [α]_D=−31.68 (*c*=2.02, CHCl₃); LRMS=264.1 [M+H].

Benzyl (2*R*,5*R*)-5-{[(5-fluoropyridin-2-yl)oxy]methyl}-2-methylpiperidine-1-carboxylate (29): A solution of **24** (120 mg, 0.456 mmol), 5-fluoro-2-hydroxypyridine (56.7 mg, 0.501 mmol), and resin-bound Ph₃P (0.254 mg, 0.547 mmol, 2.15 mmol g^{−1}) in CH₂Cl₂ (3 mL) was treated with DIAD (0.106 mL, 0.547 mmol). The mixture was stirred overnight and filtered, and the filtrate was concentrated. The crude material was purified by gradient elution RP HPLC [5→95% CH₃CN in H₂O (0.1% TFA)] to give pure fractions, which were concentrated, diluted with EtOAc, and washed with saturated aqueous NaHCO₃. The organic phase was dried over Na₂SO₄, filtered, and concentrated to yield **29** as a colorless film (107 mg, 66%). Please see figures at the end of the Supporting Information for reproductions of 500 MHz ¹H and 100.5 MHz ¹³C NMR spectra in CDCl₃ at 25 °C. [α]_D=−9.94 (*c*=2.52, CHCl₃); LRMS=359.1 [M+H].

[(2*R*,5*R*)-5-{[(5-Fluoropyridin-2-yl)oxy]methyl}-2-methylpiperidin-1-yl](2-iodo-5-methylphenyl)methanone (30): A solution of **29** (107 mg, 0.299 mmol) in EtOH (5 mL) was treated with 10 mol% Pd(OH)₂ (20.96 mg, 0.030 mmol). The flask was evacuated and backfilled with H_{2(g)} three times and stirred under a H_{2(g)} atmosphere (1 atm) at room temperature for 40 min. The mixture was filtered through a syringe filter. The filtrate was concentrated to yield desired amine, which was taken on without further purification. A solution of the crude amine (290 mg, 1.293 mmol) in DMF (5 mL) was treated with 2-iodo-5-methylbenzoic acid (339 mg, 1.293 mmol), EDC (297 mg, 1.552 mmol), HOBT (238 mg, 1.552 mmol), and TEA (0.541 mL, 3.88 mmol). After stirring at room temperature overnight, the mixture was diluted with EtOAc and

washed with H₂O twice. The organic phase was dried over Na₂SO₄, filtered, and concentrated. The crude material was purified by gradient elution on silica gel (0→50% EtOAc in hexanes) to yield **30** as a colorless oil (529 mg, 87%) over two steps. Please see figures at the end of the Supporting Information for reproductions of 500 MHz ¹H and 100.5 MHz ¹³C NMR spectra in CDCl₃ at 25 °C. [α]_D=−32.1 (*c*=2.71, CHCl₃); LRMS=468.9 [M+H].

[(2*R*,5*R*)-5-{[(5-Fluoropyridin-2-yl)oxy]methyl}-2-methylpiperidin-1-yl][5-methyl-2-(pyrimidin-2-yl)phenyl]methanone (28; MK-6096): A solution of **30** (50 mg, 0.107 mmol) in DMF (1 mL) was treated with 2-(tributylstannyl)pyrimidine (99 mg, 0.267 mmol), CsF (32.4 mg, 0.214 mmol), CuI (4.07 mg, 0.021 mmol), and (Ph₃P)₄Pd (12.34 mg, 10.68 μmol). The mixture was heated at 100 °C and stirred for 1 h. The mixture was cooled to room temperature, diluted with EtOAc, and washed with H₂O. The organic phase was concentrated and was purified by gradient elution RP HPLC [5→95% CH₃CN in H₂O (0.1% TFA)] to give pure fractions which were concentrated, diluted with EtOAc, and washed with saturated aqueous NaHCO₃. The organic phase was dried over Na₂SO₄, filtered, and concentrated to yield **28** as a white solid (26 mg, 58%); mp: 134.8 °C; [α]_D=−37.24 (*c*=3.84, CHCl₃); Compound **28** exists as a mixture of four rotameric components in chemical exchange in CDCl₃ at room temperature (74:16:7:3). ¹H and ¹³C chemical shifts of the two most populated rotamers were assigned from the analysis of COSY, HSQC, and HMBC spectra acquired on a sample dissolved in CDCl₃ at 25 °C.

Rotamer 1: (74% of total) ¹H NMR (599.458 MHz, CDCl₃, 25 °C): δ=8.75 (2H), 8.24 (1H), 8.00 (1H), 7.32 (1H), 7.19 (2H), 6.95 (1H), 6.39 (1H), 5.04 (1H), 4.36 (1H), 4.09 (1H), 3.48 (1H), 3.09 (1H), 1.99 (1H), 1.97 (2H), 1.92 (3H), 1.63 (1H), 1.50 (1H), 1.35 ppm (3H); ¹³C NMR (150.742 MHz, CDCl₃, 25 °C): δ=172.4, 164.0, 159.8, 156.8, 155.2, 141.0, 137.7, 133.1, 131.8, 129.3, 129.2, 128.3, 118.9, 111.6, 65.5, 43.9, 41.6, 32.6, 25.4, 20.9, 20.9, 14.0 ppm.

Rotamer 2: (16% of total) ¹H NMR (599.458 MHz, CDCl₃, 25 °C): δ=8.92 (2H), 8.26 (1H), 7.99 (1H), 7.35 (1H), 7.29 (1H), 7.15 (1H), 7.10 (1H), 6.77 (1H), 4.74 (1H), 4.53 (2H), 3.86 (1H), 3.12 (1H), 2.42 (3H), 2.34 (1H), 1.92 (1H), 1.89 (1H), 1.78 (1H), 1.22 (1H), 1.21 ppm (3H); ¹³C NMR (150.742 MHz, [D₆]DMSO, 25 °C): δ=171.4, 164.2, 160.1, 156.9, 156.9, 155.3, 140.4, 137.6, 133.3, 132.0, 129.7, 129.5, 127.6, 126.7, 112.0, 66.2, 49.8, 37.0, 33.0, 25.6, 21.5, 19.9, 16.1 ppm. See the Supporting Information for reproductions of ¹H and ¹³C NMR spectra. IR (KBr): ν=2978, 2940, 1619, 1567, 1485, 1414, 1265, 1224, 1013, 770 cm^{−1}; HRMS calcd for C₂₄H₂₅FN₄O₂ [M+H]: 421.2035, found: 421.2044.

The Supporting Information also includes experimental details for the syntheses of compounds **7**, **8**, **14**, **15**, **16**, **17**, **18**, **24**, **25**, **26**, and **27**.

Acknowledgements

The authors thank Professor David A. Evans for helpful synthetic chemistry discussions. We also thank Dr. Chuck Ross and Ms. Joan Murphy for HRMS analysis, Broc Flores and Laura Vasallo for synthetic support, and Dr. Chris Culberson for modeling studies on compound **4**.

Keywords: insomnia • medicinal chemistry • neurotransmitters • orexins • receptors

- [1] R. M. Benca, *Psychiatr. Serv.* **2005**, *56*, 332–343.
- [2] N. S. Kamel, J. K. Gammack, *Am. J. Med.* **2006**, *119*, 463–469.
- [3] C. L. Drake, T. Roehrs, T. Roth, *Depress. Anxiety* **2003**, *18*, 163–176.
- [4] A. Palomer, M. Prinep, A. Guglietta, *Ann. Rep. Med. Chem.* **2007**, *42*, 63–80.
- [5] G. Zammit, *Drug Safety* **2009**, *32*, 735–748.
- [6] a) L. De Lecea, T. S. Kilduff, C. Peyron, X.-B. Gao, P. E. Foye, P. E. Danielson, C. Fukuhara, E. L. F. Battenberg, V. T. Gautvik, F. S. Bartlett II, W. N. Frankel, A. N. Van Den Pol, F. E. Bloom, K. M. Gautvik, J. G. Sutcliffe, *Proc. Natl. Acad. Sci. USA* **1998**, *95*, 322–327; b) T. Sakurai, A. Amemiya, M. Ishii, I. Matsuzaki, R. Chemelli, H. Tanaka, S. C. Williams, J. A. Richardson, G. P. Kozlowski, S. Wilson, J. R. S. Arch, R. E. Buckingham, A. C. Haynes, S. A. Carr, R. S. Annan, D. E. McNulty, W. Liu, J. A. Terrell, N. A. Elshourbagy, D. J. Bergsma, M. Yanagisawa, *Cell* **1998**, *92*, 573–585.
- [7] L. Lin, J. Faraco, R. Li, H. Kadotani, W. Rogers, X. Lin, X. Qiu, P. J. de Jong, S. Nishino, E. Mignot, *Cell* **1999**, *98*, 365–376.
- [8] T. C. Thannickal, R. Y. Moore, R. Nienhuis, L. Ramanathan, S. Gulyani, M. Aldrich, M. Cornford, J. M. Siegel, *Neuron* **2000**, *27*, 469–474.
- [9] R. M. Chemelli, J. T. Willie, C. M. Sinton, J. K. Elmquist, T. Scammell, C. Lee, J. A. Richardson, S. C. Williams, Y. Xiong, Y. Kisanuki, T. E. Fitch, M. Nakazato, R. E. Hammer, C. B. Saper, M. Yanagisawa, *Cell* **1999**, *98*, 437–451.
- [10] S. P. Grady, S. Nishino, C. A. Czeisler, D. Hepner, T. E. Scammell, *Sleep* **2006**, *29*, 295–297.
- [11] a) S. A. Deadwyler, L. Porrino, J. M. Siegel, R. E. Hampson, *J. Neurosci.* **2007**, *27*, 14239–14247; b) N. Fujiki, Y. Yoshida, B. Ripley, E. Mignot, S. Nishino, *Sleep* **2003**, *26*, 953–959; c) C. J. Winrow, A. L. Gotter, C. D. Cox, S. M. Doran, P. L. Tannenbaum, M. J. Breslin, S. L. Garson, S. V. Fox, C. M. Harrell, J. Stevens, D. R. Reiss, D. Cui, P. J. Coleman, J. J. Renger, *J. Neurogenet.* **2011**, *25*, 52–61.
- [12] a) T. E. Scammell, C. D. Winrow, *Ann. Rev. Pharm. Toxicol.* **2011**, *51*, 243–266; b) J. Gatfield, C. Brisbare-Roch, F. Jenck, C. Boss, *ChemMedChem* **2010**, *5*, 1197–1214; c) P. J. Coleman, J. J. Renger, *Expert Opin. Ther. Pat.* **2010**, *20*, 307–324.
- [13] C. D. Cox, M. J. Breslin, D. B. Whitman, J. D. Schreier, G. B. McGaughey, M. J. Bogusky, A. J. Roecker, S. P. Mercer, R. A. Bednar, W. Lemaire, J. G. Bruno, D. R. Reiss, C. M. Harrell, K. L. Murphy, S. L. Garson, S. M. Doran, T. Prueksaritanont, W. B. Anderson, C. Tang, S. Roller, T. D. Cabalu, D. Cui, G. D. Hartman, S. D. Young, K. S. Koblan, C. J. Winrow, J. J. Renger, P. J. Coleman, *J. Med. Chem.* **2010**, *53*, 5320–5332.
- [14] W. J. Herring, K. S. Budd, J. Hutzelmann, E. Snyder, D. Snavely, K. Liu, C. Lines, D. Michelson, T. Roth, *Sleep* **2010**, *33*, Abstract Supplement 2010.
- [15] D. B. Whitman, C. D. Cox, M. J. Breslin, K. M. Brashear, J. D. Schreier, M. J. Bogusky, R. A. Bednar, W. Lemaire, J. G. Bruno, G. D. Hartman, D. R. Reiss, C. M. Harrell, R. L. Kraus, Y. Li, S. L. Garson, S. M. Doran, T. Prueksaritanont, C. Li, C. J. Winrow, K. S. Koblan, J. J. Renger, P. J. Coleman, *ChemMedChem* **2009**, *4*, 1069–1074.
- [16] C. Brisbare-Roch, J. Dingemanse, R. Koberstein, P. Hoever, H. Aissaoui, S. Flores, C. Mueller, O. Nayler, J. Van Gerven, S. L. Haas, P. Hess, C. Qiu, S. Buchmann, M. Scherz, T. Weller, W. Fischli, M. Clozel, F. Jenck, *Nat. Med.* **2007**, *13*, 150–155.
- [17] P. Bettica, G. Nucci, C. Pyke, L. Squassante, S. Zamuner, E. Ratti, R. Gomeni, R. Alexander, *J. Psychopharmacol.* **2011**, DOI: 10.1177/0269881111408954.
- [18] R. Di Fabio, A. Pellacani, S. Faedo, A. Roth, L. Piccoli, P. Gerrard, R. A. Porter, C. N. Johnson, K. Thewlis, D. Donati, L. Stasi, S. Spada, G. Stemp, D. Nash, C. Branch, L. Kindon, M. Leanda, M. Massagrande, A. Poffe, B. Alessandro, S. Braggio, E. Chiarparin, C. Marchioro, E. Ratti, M. Corsi, *Bio. Org. Med. Chem. Lett.* **2011**, *21*, 5562–5567.
- [19] P. Gaillard, C. N. Johnson, R. Novelli, R. A. Porter, G. Stemp, K. M. Thewlis, WO 2002089800, **2002**, 34 pp.
- [20] P. J. Coleman, C. D. Cox, A. J. Roecker, *Curr. Top. Med. Chem.* **2011**, *11*, 696–725.
- [21] a) E. E. Sugg, J. F. Griffin, P. S. Portoghese, *J. Org. Chem.* **1985**, *50*, 5032–5037; b) H. Paulsen, K. Todt, *Angew. Chem.* **1966**, *78*, 943–944; *Angew. Chem. Int. Ed. Engl.* **1966**, *5*, 899–900; c) F. Johnson, *Chem. Rev.* **1968**, *68*, 375–413.
- [22] The axial conformer of **4** is calculated to be 7.3 kcal mol⁻¹ more stable than the conformer with an equatorial α substituent. Conformations for **4** were generated by using a combination of Omega (OpenEye) and et/jg (B. Feuston—personal communication); subsequent conformations were minimized using MacroModel (Schrödinger) with the MMFF force field using a 2*r* distance-dependent dielectric.
- [23] C. D. Cox, G. B. McGaughey, M. J. Bogusky, D. B. Whitman, R. G. Ball, C. J. Winrow, J. J. Renger, P. J. Coleman, *Bioorg. Med. Chem. Lett.* **2009**, *19*, 2997–3001.
- [24] a) P. J. Coleman, J. D. Schreier, G. B. McGaughey, M. J. Bogusky, C. D. Cox, G. D. Hartman, R. G. Ball, C. M. Harrell, D. R. Reiss, T. Prueksaritanont, C. J. Winrow, J. J. Renger, *Bioorg. Med. Chem. Lett.* **2010**, *20*, 2311–2315; b) P. J. Coleman, J. D. Schreier, A. J. Roecker, S. P. Mercer, G. B. McGaughey, C. D. Cox, G. D. Hartman, C. M. Harrell, D. R. Reiss, S. M. Doran, S. L. Garson, W. B. Anderson, C. Tang, T. Prueksaritanont, C. J. Winrow, J. J. Renger, *Bioorg. Med. Chem. Lett.* **2010**, *20*, 4201–4205.
- [25] Replacing the phenylthiazoyl carboxamide with 2-(2H-1,2,3-triazol-2-yl)-5-methylbenzamide improves physicochemical properties and orexin binding affinity.
- [26] For preparation of 2-(2H-1,2,3-triazol-2-yl)-5-methylbenzoic acid, see ref. [12].
- [27] In related occupancy experiments in rat, higher unbound plasma concentration correlated with higher CSF levels of drug.
- [28] Compound **28**: $C_{24}H_{25}FN_4O_2$, $M_r = 420.480$, monoclinic, $P2_1$, $a = 10.8883(9)$, $b = 17.8183(15)$, $c = 12.0063(10)$ Å, $\beta = 116.2840(10)$ °, $V = 2088.5(3)$ Å³, $Z = 4$, $D_x = 1.337$ g cm⁻³, monochromatized radiation $\lambda(Mo) = 0.71073$ Å, $\mu = 0.09$ mm⁻¹, $F(000) = 888$, $T = 100$ K. Data were collected on a Bruker CCD diffractometer to a θ limit of 28.34°, which yielded 23849 reflections. There are 9455 unique reflections with 9112 observed at the 2σ level. The structure was solved by direct methods (SHELXS-97, G. M. Sheldrick, *Acta Crystallogr. Sect. A Found. Crystallogr.* **2008**, *64*, 112–122) and refined using full-matrix least-squares on F^2 (SHELXL-97, G. M. Sheldrick, *Acta Crystallogr.* **2008**, *A64*, 112–122). The compound crystallized with two independent molecules in the asymmetric unit of the lattice. The final model was refined using 563 parameters and all 9455 data. All non-hydrogen atoms were refined with anisotropic thermal displacements. The final agreement statistics are: $R = 0.035$ (based on 9112 reflections with $I > 2\sigma(I)$), $wR = 0.088$, $S = 1.03$ with $(\Delta/\sigma)_{\text{max}} < 0.01$. The maximum peak height in a final difference Fourier map is 0.219 e Å⁻³, and this peak is without chemical significance. CCDC-857980 contains the supplementary crystallographic data for this paper. These data can be obtained free of charge from The Cambridge Crystallographic Data Centre via www.ccdc.cam.ac.uk/data_request/cif.
- [29] C. J. Winrow, A. L. Gotter, C. D. Cox, P. L. Tannenbaum, S. L. Garson, S. M. Doran, M. J. Breslin, J. D. Schreier, S. V. Fox, C. M. Harrell, J. Stevens, D. R. Reiss, D. Cui, P. J. Coleman, J. J. Renger, *Neuropharm.* **2011**, *62*, 978–987.
- [30] Compound **28** was tested for its effect on hERG channels heterologously expressed in CHO K1 cells using standard whole-cell voltage-clamp techniques. Compound **28** inhibited hERG current with an IC_{50} value of 46 μM.
- [31] Compound **28** was administered intravenously over three sequential 30-min periods at 1, 5, and 6 mg kg⁻¹ in a vehicle of 30% (w/v) hydroxypropyl-β-cyclodextrin in water to determine its effects on cardiovascular function in three anesthetized, vagotomized dogs. These effects were compared with vehicle previously tested in a separate set of four dogs. Heart rate, mean arterial pressure, and electrocardiographic parameters (PR, QRS, and QT/QTC intervals) were monitored predose and during each 30-min infusion period. No treatment-related effects were observed. Peak compound **28** plasma concentrations (mean) measured during the 30-min infusions of 1, 5, and 6 mg kg⁻¹ were 4, 13, and 19 μM, respectively.
- [32] For a description of the occupancy assay, see ref. [11c].
- [33] K. M. Connor, E. Mahoney, S. Jackson, J. Hutzelmann, X. Zhao, E. Snyder, D. Snavely, D. Michelson, T. Roth, W. J. Herring, *Sleep Biol. Rhythms* **2011**, *9*, 332.

Received: January 13, 2012

Published online on February 3, 2012